

We are IntechOpen, the world's leading publisher of Open Access books Built by scientists, for scientists

6,900

Open access books available

186,000

International authors and editors

200M

Downloads

Our authors are among the

154

Countries delivered to

TOP 1%

most cited scientists

12.2%

Contributors from top 500 universities



WEB OF SCIENCE™

Selection of our books indexed in the Book Citation Index
in Web of Science™ Core Collection (BKCI)

Interested in publishing with us?
Contact book.department@intechopen.com

Numbers displayed above are based on latest data collected.
For more information visit www.intechopen.com



Physics of Absorption and Generation of Electromagnetic Radiation

Sukhmander Singh, Ashish Tyagi and Bhavna Vidhani

Abstract

The chapter is divided into two parts. In the first part, the chapter discusses the theory of propagation of electromagnetic waves in different media with the help of Maxwell's equations of electromagnetic fields. The electromagnetic waves with low frequency are suitable for the communication in sea water and are illustrated with numerical examples. The underwater communication have been used for the oil (gas) field monitoring, underwater vehicles, coastline protection, oceanographic data collection, etc. The mathematical expression of penetration depth of electromagnetic waves is derived. The significance of penetration depth (skin depth) and loss angle are clarified with numerical examples. The interaction of electromagnetic waves with human tissue is also discussed. When an electric field is applied to a dielectric, the material takes a finite amount of time to polarize. The imaginary part of the permittivity is corresponds to the absorption length of radiation inside biological tissue. In the second part of the chapter, it has been shown that a high frequency wave can be generated through plasma under the presence of electron beam. The electron beam affects the oscillations of plasma and triggers the instability called as electron beam instability. In this section, we use magnetohydrodynamics theory to obtain the modified dispersion relation under the presence of electron beam with the help of the Poisson's equation. The high frequency instability in plasma grow with the magnetic field, wave length, collision frequency and the beam density. The growth rate linearly increases with collision frequency of electrons but it is decreases with the drift velocity of electrons. The real frequency of the instability increases with magnetic field, azimuthal wave number and beam density. The real frequency is almost independent with the collision frequency of the electrons.

Keywords: electromagnetic waves, permittivity, skin depth, loss angle, absorption, Dispersion equations, electron collisions, growth rate, Hall thruster, beam, resistive instability

1. Introduction

X-rays are used to detect bone fracture and determine the crystals structure. The electromagnetic radiation are also used to guide airplanes and missile systems. Gamma rays are used in radio therapy for the treatment of cancer and tumor. Gamma rays are used to produce nuclear reaction. The earth get heat from Infrared waves. It is used to kill microorganism. Ultraviolet rays are used for the sterilizing of

The Electromagnetic Spectrum				
Frequency (Hz)	Nature	Wavelength (m)	Production	Applications
10^{22}	gamma rays	10^{-13}	Nuclear decay	Cosmic rays
10^{21}	gamma rays	10^{-12}	Nuclear decay	Cancer therapy
10^{18}	x rays	10^{-9}	Inner electronic transitions and fast collisions	Medical diagnosis
10^{16}	ultraviolet	10^{-7}		Sterilization
10^{15}	visible	10^{-6}	Thermal agitation and electronic transitions	Vision, astronomy, optical
6.5×10^{14}	blue	4.6×10^{-7}		
5.6×10^{14}	green	5.4×10^{-7}		
3.9×10^{14}	red	7.6×10^{-7}		
10^{14}	infrared	10^{-5}	Thermal agitation and electronic transitions	Heating, night vision, optical communications
10^9	UHF	10^{-3}	Accelerating charges and thermal agitation	Microwave ovens
10^{10}	EHF	10^{-1}		Remote sensing
10^8	TV FM	10		Radio transmission
10^6	AM	10^3		Radio signals
10^4	RF	10^5	Accelerating charges	

Table 1.
The electromagnetic spectrum.

surgical instruments. It is also used for study molecular structure and in high resolving power microscope. The color of an object is due to the reflection or transmission of different colors of light. For example, a fire truck appears red because it reflects red light and absorbs more green and blue wavelengths. Electromagnetic waves have a huge range of applications in broadcasting, WiFi, cooking, vision, medical imaging, and treating cancer. Sequential arrangement of electromagnetic waves according to their frequencies or wave lengths in the form of distinct of groups having different properties in called electromagnetic spectrum. In this section, we discuss how electromagnetic waves are classified into categories such as radio, infrared, ultraviolet, which are classified in **Table 1**. We also summarize some of the main applications for each range of electromagnetic waves. Radio waves are commonly used for audio communications with wavelengths greater than about 0.1 m. Radio waves are produced from an alternating current flowing in an antenna.

2. Current status of the research

Underwater communications have been performed by acoustic and optical systems. But the performance of underwater communications is affected by multipath propagation in the shallow water. The optical systems have higher propagation speed than underwater acoustic waves but the strong backscattering due to suspended particles in water always limits the performance of optical systems [1]. UV radiation, free radicals and shock waves generated from electromagnetic fields

are effectively used to sterilize bacteria. Pulsed electromagnetic fields (streamer discharge) in water are employed for the sterilization of bacteria. For biological applications of pulsed electromagnetic field, electroporation is usually used to sterilize bacteria. This technique is commonly applied for sterilization in food processing. The cells in the region of tissue hit by the laser beam (high intensities $\sim 10 - 100 \text{ W/cm}^2$) usually dies and the resulting region of tissue burn is called a photocoagulation burn. Photocoagulation burns are used to destroy tumors, treat eye conditions and stop bleeding.

Electromagnetic waves in the RF range can also be used for underwater wireless communication systems. The velocity of EM waves in water is more than 4 orders faster than acoustic waves so the channel latency is greatly reduced. In addition, EM waves are less sensitive than acoustic waves to reflection and refraction effects in shallow water. Moreover, suspended particles have very little impact on EM waves. Few underwater communication systems (based on EM waves) have been proposed in reference [2, 3]. The primary limitation of EM wave propagation in water is the high attenuation due to the conductivity of water. For example, it has been shown in [4] that conventional RF propagation works poorly in seawater due to the losses caused by the high conductivity of seawater (typically, 4 S/m). However, fresh water has a typical conductivity of only 0.01 S/m, which is 400 times less than the typical conductivity of seawater. Therefore, EM wave propagation can be more efficient in fresh water than in seawater. Jiang, and Georgakopoulos analyzed the propagation and transmission losses for a plane wave propagating from air to water (frequency range of 23 kHz to 1 GHz). It has been depicted that the propagation loss increases as the depth increases, whereas the transmission loss remains the same for all propagation depths [5]. Mazharimousavi et al. considered variable permeability and permittivity to solve the wave equation in material layers [6]. The Compton and Raman scattering effects are widely employed in the concept of free electron lasers. These nonlinear effects have great importance for fusion physics, laser-plasma acceleration and EM-field harmonic generation. Matsko and Rostovtsev investigated the behavior of overdense plasmas in the presence of the Electromagnetic fields, which can lead to the nonlinear effects such as Raman scattering, modulational instability and self-focusing [7]. The increasing relativistic mass of the particles can make plasma transparent in the presence of high intense the electromagnetic field change the properties of plasmas [8]. The models of electromagnetic field generated in a non absorbing anisotropic multilayer used to study the optical properties of liquid crystals and propagation of electromagnetic waves in magneto active plasmas [9]. Pulse power generator based on electromagnetic theory has applications such as water treatment, ozone generation, food processing, exhaust gas treatment, engine ignition, medical treatment and ion implantation. The similar work was reviewed by Akiyama et al. [10]

Applications for environmental fields involving the decomposition of harmful gases, generation of ozone, and water treatment by discharge plasmas in water utilizing pulsed power discharges have been studied [11–14]. High power microwave can be involved to joining of solid materials, to heat a surface of dielectric material and synthesis of nanocomposite powders. Bruce et al. used a high-power millimeter wave beam for joining ceramics tubes with the help of 83-GHz Gyrotron [15]. The use of shock waves to break up urinary calculi without surgery, is called as extracorporeal shock wave lithotripsy. Biofilm removal to inactivation of fungi, gene therapy and oncology are the interesting uses of shock waves lithotripsy. Loske overviewed the biomedical applications (orthopedics, cardiology, traumatology, rehabilitation, esthetic therapy) of shock waves including some current research. [16]. Watts et al. have reported the theory, characterization and fabrications of metamaterial perfect absorbers (MPAs) of electromagnetic waves. The motivation

for studying MPAs comes mainly from their use in potential applications as selective thermal emitters in automotive radar, in local area wireless network at the frequency range of 92–95 GHz and in imaging at frequency 95 and 110 GHz. [17]. Ayala investigated the applications of millimeter waves for radar sensors [18]. Metamaterial perfect absorbers are useful for spectroscopy and imaging, actively integrated photonic circuits and microwave-to-infrared signature control [19–21]. In [22, 23], authors show the importance of THz pulse imaging system for characterizing biological tissues such as skin, muscle and veins. Reference [24] reported the propagation of EM waves on a graphene sheet. The Reference [25] compared the CNT-based nano dipole antenna and GNR-based nano patch antenna. Due to short wavelength, even a minute variations in water contents and biomaterial tissues can be detected by terahertz radiations due to existence of molecular resonances at such frequencies. Consequently, one of the emerging areas of research is analyzing the propagation of terahertz electromagnetic waves through the tissues to develop diagnostic tools for early detection and treatment such as abnormalities in skin tissues as a sign of skin cancer [26]. Shock waves may stimulate osteogenesis and chondrogenesis effects [27], induce analgesic effects [28] and tissue repair mechanisms [29]. Shock waves therapy are also used to treat oncological diseases and other hereditary disorders [27, 30]. Chen et al. proposed a mathematical model for the propagating of electromagnetic waves coupling for deep implants and simulated through COMSOL Multiphysics [31]. Body area networks technological is used to monitor medical sensors implanted or worn on the body, which measure important physical and physiological parameters [32, 33]. Marani and Perri reviewed the aspects of Radio Frequency Identification technology for the realization of miniaturized devices, which are implantable in the human body [34]. Ultrasonic can transport high power and can penetrate to a deeper tissue with better power efficiency. [35, 36]. Ref. [37], discuss the radar-based techniques to detect human motions, wireless implantable devices and the characterization of biological materials. Low frequency can deliver more power with deeper penetrating ability in tissue [38, 39]. Contactless imaging techniques based on electromagnetic waves are under continuous research. Magnetic resonance imaging technology and physiological processes of biological tissues and organisms [40, 41]. The electrical properties of biological mediums are found very useful because it is related to the pathological and physiological state of the tissues [42–44].

3. Interaction of electromagnetic wave fields with biological tissues

From last decade, researchers are interested about biological effects of electromagnetic energy due to public concern with radiation safety and measures. The electromagnetic energy produces heating effects in the biological tissues by increasing the kinetic energy of the absorbing molecules. Therefore the body tissues absorb strongly in the UV and in the Blue/green portion of the spectrum and transmit reds and IR. A surgeon can select a particular laser to target cells for photovaporization by determining which wavelengths your damaged cell will absorb and what the surrounding tissue will not. The heating of biological tissues depends on dielectric properties of the tissues, tissue geometry and frequency of the source. The tissues of the human body are extremely complex. Biological tissues are composed of the extracellular matrix (ECM), cells and the signaling systems. The signaling systems are encoded by genes in the nuclei of the cells. The cells in the tissues reside in a complex extracellular matrix environment of proteins, carbohydrates and intracellular fluid composed of several salt ions, polar water molecules and polar protein molecules. The dielectric constant of tissues decreases as the

frequency is increased to GHz level. The effective conductivity, rises with frequency. The tissues of brain, muscle, liver, kidney and heart have larger dielectric constant and conductivity as compared to tissues of fat, bone and lung. The action of electromagnetic fields on the tissues produce the rotation of dipole molecules at the frequency of the applied electromagnetic energy which in turn affects the displacement current through the medium with an associated dielectric loss due to viscosity. The electromagnetic field also produce the oscillation of the free charges, which in turn gives rise to conduction currents with an associated energy loss due to electrical resistance of the medium. The interaction of electromagnetic wave fields with biological tissues is related to dielectric properties. Johnson and Guy reviewed the absorption and scattering effects of light in biological tissues [45]. In ref. [46], the method of warming of human blood from refrigerated (bank blood storage temperature ~ 4 to 6°C) has been discussed with the help of microwave.

4. Complex dielectric permittivity

The dielectric permittivity of a material is a complex number containing both real and imaginary components. It describes a material's ability to permit an electric field. It dependent on the frequency, temperature and the properties of the material. This can be expressed by

$$\epsilon_c = \epsilon_0(\epsilon' - j\epsilon'') \quad (1)$$

where ϵ' is the dielectric constant of the medium. The ϵ'' is called the loss factor of the medium and related with the effective conductivity such that $\epsilon'' = \frac{\sigma}{\epsilon_0\omega}$. These coefficients are related through by loss tangent $\tan \delta = \frac{\epsilon''}{\epsilon'}$. In other words loss factor is the product of loss tangent and dielectric constant, that is $\epsilon'' = \epsilon' \tan \delta$. The loss tangent depends on frequency, moisture content and temperature. If all energy is dissipated and there is no charging current then the loss tangent would tend to infinity and if no energy is dissipated, the loss tangent is zero [45, 47–49]. The high power electromagnetic waves are used to generate plasma through laser plasma interaction. Gaseous particles are ionized to bring it in the form of plasma through injection of high frequency microwaves. The electrical permittivity in plasma is affected by the plasma density [50]. If the microwave electric field (\tilde{E}) and the velocity (\tilde{v}) are assumed to be varying with $e^{i\omega t}$, the plasma dielectric constant can be read as,

$$\epsilon = \epsilon_0 \left(1 - \frac{\omega_{pe}^2}{\omega^2} \right) \quad (2)$$

Where; the ω_{pe} is the electron plasma frequency and given by the relation,

$$\omega_{pe} = \sqrt{\frac{n_e e^2}{\epsilon_0 m_e}} \quad (3)$$

Recently many researchers have studied the plasma instabilities in a crossed field devices called Hall thrusters (space propulsion technology). The dispersion relations for the low and high frequency electrostatic and electromagnetic waves are derived in the magnetized plasma. The dispersion relations for the resistive and Rayleigh Taylor instabilities has been derived for the propagation of waves in a magnetized plasma under the effects of various parameters [51–61].

5. Propagation of EM fields (waves) in conductors

The behavior of EM waves in a conductor is quite different from that in a source-free medium. The conduction current in a conductor is the cause of the difference. We shall analyze the source terms in the Maxwell's equations to simplify Maxwell's equations in a conductor. From this set of equations, we can derive a diffusion equation and investigate the skin effects.

5.1 Gauss' law for electric field

The Electric flux φ_E through a closed surface A is proportional to the net charge q enclosed within that surface.

$$\varphi_E = \oint \vec{E} \cdot \hat{n} dA = \frac{q}{\epsilon_0} = \frac{1}{\epsilon_0} \int_V \rho dV \quad (4)$$

$$\text{Differential form, } \vec{\nabla} \cdot \vec{E} = \frac{\rho}{\epsilon_0} \quad (5)$$

5.2 Faraday's law

The electromagnetic force induced in a closed loop, is proportional to the negative of the rate of change of the magnetic flux, φ_B through the closed loop,

$$\oint \vec{E} \cdot d\vec{l} = -\frac{\partial \varphi_B}{\partial t} = -\frac{\partial}{\partial t} \oint \vec{B} \cdot dA \quad (6)$$

Faraday's law in differential form,

$$\vec{\nabla} \times \vec{E} = -\frac{\partial \vec{B}}{\partial t} \quad (7)$$

5.3 Magnetic Gauss's law for magnetic field

The Magnetic flux φ_B through a closed surface, A is equal to zero.

$$\varphi_B = \oint \vec{B} \cdot dA = 0 \quad (8)$$

In the differential form

$$\vec{\nabla} \cdot \vec{B} = 0 \quad (9)$$

5.4 Ampere's law

The path integral of the magnetic field around any closed loop, is proportional to the current enclosed by the loop plus the displacement current enclosed by the loop.

$$\oint \vec{B} \cdot d\vec{l} = \mu_0 I + \mu_0 \epsilon_0 \frac{\partial \varphi_E}{\partial t} \quad (10)$$

Ampere's law in differential form

$$\vec{\nabla} \times \vec{B} = \mu_0 \vec{J} + \mu_0 \epsilon_0 \frac{\partial \vec{E}}{\partial t} \quad (11)$$

6. Properties of plane wave (monochromatic) in vacuum

Let us assume that the wave equations (fields) has the solution in the form of $\vec{E}(\vec{B}) = \vec{E}_0(\vec{B}_0)e^{-i(kz-\omega t)}$, then the vector operators can be written as $\nabla \rightarrow -ik$ and $\frac{\partial}{\partial t} \rightarrow i\omega$.

a. The vector k and fields $\vec{E}(\vec{B})$ are perpendicular

From Gauss's law $k \cdot E = 0$

b. The field \vec{B} is perpendicular to the vector k and field \vec{E}

From Faraday's law $-i\vec{k} \times \vec{E} = -i\omega\vec{B}$

$$\Rightarrow \vec{B} = \frac{\vec{k} \times \vec{E}}{\omega} = \frac{k\hat{k} \times \vec{E}}{\omega} = \frac{\hat{k} \times \vec{E}}{c} \quad (12)$$

Where we have used $\omega = ck$ and unit vector $\hat{k} = \vec{k}/k$. This implies that all three vectors are perpendicular to one another (**Figure 1**).

Let us apply curl operator to the 2nd equation.

Maxwell's equation:

$$\vec{\nabla} \times (\vec{\nabla} \times \vec{E}) = -\vec{\nabla} \times \left(\frac{\partial \vec{B}}{\partial t} \right) = -\frac{\partial}{\partial t} (\vec{\nabla} \times \vec{B}) = -\frac{\partial}{\partial t} \left(\mu\sigma\vec{E} + \mu\epsilon\frac{\partial \vec{E}}{\partial t} \right) \quad (13)$$

So

$$-\nabla^2\vec{E} = -\mu\sigma\frac{\partial \vec{E}}{\partial t} - \mu\epsilon\frac{\partial^2 \vec{E}}{\partial t^2} \quad (14)$$

Similar, the magnetic field satisfy the same equation

$$-\nabla^2\vec{B} = -\mu\sigma\frac{\partial \vec{B}}{\partial t} - \mu\epsilon\frac{\partial^2 \vec{B}}{\partial t^2} \quad (15)$$

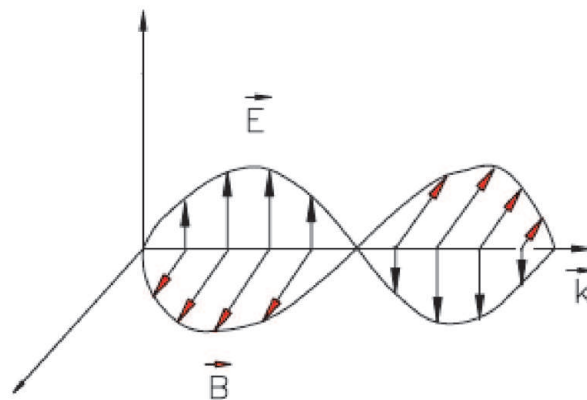


Figure 1.
 Orientations of electric field, magnetic field and wave vector.

6.1 Skin depth

Suppose we have a plane wave field. It comes from the $-z$ direction and reaches a large conductor. Surface at $z = 0$ outside of a conductor: $E = E_0 e^{-i\omega t} e_x$ at $z = 0$. Looking for the wave like solution of electric (magnetic) fields by assuming the wave inside the conductor has the form, where k is an unknown constant. Suppose, the waves are traveling only in the z direction (no x or y components). These waves are called plane waves, because the fields are uniform over every plane perpendicular to the direction of propagation. We are interested, then, in fields of the form

$$\vec{E}(\vec{B}) = \vec{E}_0(\vec{B}_0) e^{-i(kz - \omega t)} \quad (16)$$

for the waves of the above type, we find from the diffusion equation

$$k^2 E = -i\omega\mu\sigma E + \mu\epsilon\omega^2 E \quad (17)$$

$$\text{Or } (k^2 + i\omega\mu\sigma - \mu\epsilon\omega^2)E = 0$$

$$\text{For non-trivial solution } k^2 + i\omega\mu\sigma - \mu\epsilon\omega^2 = 0 \quad (18)$$

The presence of imaginary term due to conductivity of the medium gives different dispersion relation from the dielectric medium. From Eq. (18) we can expect the wave vector to have complex form.

Let us write

$$\vec{k} = \vec{\alpha} - i\vec{\beta} \quad (19)$$

Here the real part $\vec{\alpha}$ determine the wavelength, refractive index and the phase velocity of the wave in a conductor. The imaginary part $\vec{\beta}$ corresponds to the skin depth in a conductor. The solutions of Eqs. (18) and (19), gives the real and imaginary part of wave vector k in terms of materials' properties.

$$\alpha = \omega \sqrt{\frac{\epsilon\mu}{2}} \left[\sqrt{1 + \frac{\sigma^2}{\epsilon^2\omega^2}} + 1 \right]^{\frac{1}{2}} \quad (20)$$

$$\text{And } \beta = \frac{\omega\mu\sigma}{2\alpha} \quad (21)$$

$$\text{Or } \beta = \omega \sqrt{\frac{\epsilon\mu}{2}} \left[\sqrt{1 + \frac{\sigma^2}{\epsilon^2\omega^2}} - 1 \right]^{\frac{1}{2}} \quad (22)$$

If we use complex wave vector $\vec{k} = \vec{\alpha} - i\vec{\beta}$ into Eq. (16), then the wave equation for a conducting medium can be written as

$$\vec{E} = \vec{E}_0 e^{-\beta z} e^{-i(\alpha z - \omega t)} \quad (23)$$

It is clear from the above equation that the conductivity of the medium affects the wavelength for a fixed frequency. The first exponential factor $e^{-\beta z}$ gives an exponential decay in the amplitude (with increasing z) of the wave as shown in **Figure 2**. The cause of the decay of the amplitude of the wave can be explained in a very precise way in terms of conservation of energy. Whenever the incoming

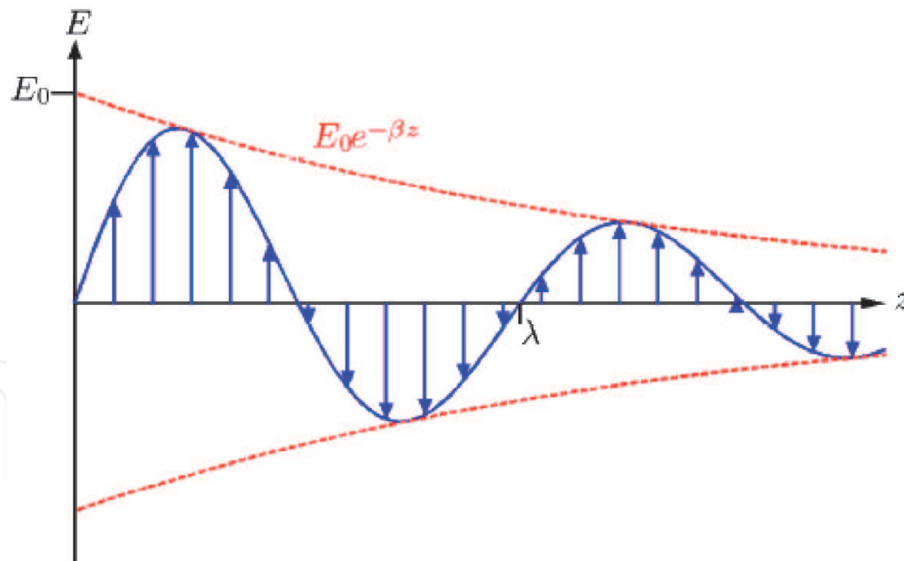


Figure 2.
 Decaying of electromagnetic field.

electromagnetic radiation interacts with a conducting material, it produces current in the in the conductor. The current produces Joule heating effect which must be compensated from the energy of the wave. Therefore we can expect the decay in the amplitude of the wave. The second factor $e^{-i(\alpha z - \omega t)}$ gives the plane wave variations with space and time.

7. Alternating magnetic field in a conducting media

From Faraday's law, the both fields are related by

$$\vec{k} \times \vec{E}_0 = \omega \vec{B}_0 \quad (24)$$

$$\text{Or } \vec{B}_0 = \frac{\vec{k} \times \vec{E}_0}{\omega} \quad (25)$$

Thus as in dielectric case, both fields are perpendicular to each other and also perpendicular to the direction of motion with same phase angle.

7.1 Phase change in fields in a conducting media

The complex wave vector k , gives the phase angle between the fields in a conducting medium. Let us assume that E is polarized along the x direction

$$\vec{E} = \hat{i} E_0 e^{-\beta z} e^{-i(\alpha z - \omega t)} \quad (26)$$

And the magnetic field results from Eq. (25) is given by

$$\vec{B} = \hat{j} \frac{|k|}{\omega} E_0 e^{-\beta z} e^{-i(\alpha z - \omega t)} \quad (27)$$

From Eq. (19), the complex number k can be written as

$$|k| = \sqrt{\alpha^2 + \beta^2} e^{i\varphi} = \text{Re } e^{i\varphi} \quad (28)$$

$$\text{Thus } R = \sqrt{\alpha^2 + \beta^2} = \omega \sqrt{\epsilon\mu} \left[\sqrt{1 + \frac{\sigma^2}{\epsilon^2 \omega^2}} \right]^{\frac{1}{4}} \quad (29)$$

$$\text{And the phase angle } \varphi = \tan^{-1} \frac{\beta}{\alpha} \quad (30)$$

Further if the initial phases of the fields are φ_E and φ_B , then the amplitude are given by

$$\vec{E}_0 = E_0 e^{i\varphi_E} \quad (31)$$

$$\vec{B}_0 = B_0 e^{i\varphi_B} \quad (32)$$

From Eq. (27)

$$B_0 e^{i\varphi_B} = \frac{\text{Re } e^{i\varphi}}{\omega} E_0 e^{i\varphi_E} \quad (33)$$

Therefore, the both fields are out of phase with angle

$$\varphi = \varphi_B - \varphi_E \quad (34)$$

From Eq. (33) the ratio of the magnetic field to the electric field is

$$\frac{B_0}{E_0} = \frac{R}{\omega} \quad (35)$$

By using Eq. (29)

$$\frac{B_0}{E_0} = \sqrt{\epsilon\mu} \left[1 + \frac{\sigma^2}{\epsilon^2 \omega^2} \right]^{\frac{1}{4}} \quad (36)$$

In other words, we can say that the magnetic field advanced from electric field by the phase angle φ . In terms of sinusoidal form, these fields follow the following expressions.

$$\vec{E} = \hat{i} \vec{E}_0 e^{-\beta z} \cos(\omega t - \alpha z + \varphi_E) \quad (37)$$

And the magnetic field results from Eq. (32) is given by

$$\vec{B} = \hat{j} \vec{B}_0 e^{-\beta z} \cos(\omega t - \alpha z + \varphi_E + \varphi) \quad (38)$$

The above equations direct that the amplitude of an electromagnetic wave propagating (through a conductor) decays exponentially on a characteristic length scale, d , that is known as the skin-depth [48].

7.2 Skin depth

Skin depth measure the distance that the wave travels before it's amplitude falls to $1/e$ of its original value [48]. From Eq. (37), the amplitude of the wave falls by a

factor $1/e$ in a distance $z = \frac{1}{\beta}$. In other words it is a measure of how far the wave penetrates into the conductor. Mathematically skin depth is denoted by δ , therefore

$$\delta = \frac{1}{\beta} \quad (39)$$

If we study poor conductor, which satisfies the inequality $\sigma \ll \epsilon\omega$, then Eqs. (20) and (21) leads to

$$\alpha \approx \omega\sqrt{\epsilon\mu} \quad (40)$$

$$\text{And we know that } \beta = \frac{\omega\mu\sigma}{2\alpha} \quad (41)$$

Substitute the value of α into Eq. (32), we get

$$\text{Or } \beta \approx \omega \frac{\mu\sigma}{2\omega\sqrt{\epsilon\mu}} \quad (42)$$

$$\text{Or } \beta \approx \frac{\sigma}{2} \sqrt{\frac{\mu}{\epsilon}} \quad (43)$$

$$\text{The phase velocity } V_{ph} = \frac{\omega}{\alpha} \approx \frac{1}{\sqrt{\epsilon\mu}} \quad (44)$$

$$\text{Skin depth in poor conductor } \delta = \frac{1}{\beta} = \frac{2}{\sigma} \sqrt{\frac{\epsilon}{\mu}} \quad (45)$$

So, it is independent from the frequency.

The Eq. (41) state that at higher frequency, the absorbing parameter lost its significance that is $\beta \ll \alpha$. We can conclude that at higher frequency the wavelength does not decay very fast in a poor conductor. Moreover both the fields are also in same phase by the relation $\omega B_0 = \alpha E_0$. Also the phase velocity is independent from the frequency [47].

8. Wave propagation in perfect conductors

The transmission lines and communication systems are made up with silver, copper and aluminum. In most cases these conductors satisfies the inequality $\sigma \gg \epsilon\omega$, then Eqs. (20) and (21) leads to

$$\alpha \approx \sqrt{\frac{\omega\mu\sigma}{2}} \quad (46)$$

$$\text{And } \beta \approx \sqrt{\frac{\omega\mu\sigma}{2}} \quad (47)$$

$$\text{Therefore } \beta \approx \alpha \quad (48)$$

$$\text{Skin depth } \delta = \frac{1}{\beta} = \frac{1}{\alpha} = \sqrt{\frac{2}{\omega\mu\sigma}} \quad (49)$$

The wave decays significantly within one wavelength. Since $\delta \propto \sqrt{1/\omega\sigma}$, the deep penetration occurs, when the inequality $\sigma \ll \epsilon\omega$ is satisfied (at Low frequency in a Poor conductor).

9. Electromagnetic wave propagation into water

EM wave propagation can be more efficient in fresh water than in seawater. The radiofrequency wave propagation works poorly in seawater due to the losses caused by the high conductivity of seawater. The limitation of EM wave propagation in water is the high attenuation due to the conductivity of water (typically, 4 S/m), however fresh water has a conductivity of 0.01 S/m. These properties are used to construct underwater sensor network based on electromagnetic waves to trace out the natural resources buried underwater, where the conventional optical water sensors are difficult to utilize in an underwater environment due to backscatter and absorptions [47].

Example:

For sea water,

$$\mu = \mu_0 = 4\pi \times 10^{-7} \text{N/A}^2, \epsilon \cong 81\epsilon_0 \text{ and } \sigma \approx 5(\Omega.m)^{-1}.$$

The skin depth in poor conductor

$$\delta = \frac{2}{\sigma} \sqrt{\frac{\epsilon}{\mu}} = \frac{2}{\sigma} \sqrt{\frac{81\epsilon_0}{\mu_0}} \quad (50)$$

$$= \frac{2\sqrt{81}}{\sigma Z} = \frac{18}{5 \times 377} \approx 0.96 \text{cm}. \quad (51)$$

If the sea water satisfies the inequality $\sigma \ll \epsilon\omega$, of poor conductor, which require

$$f = \frac{\omega}{2\pi} \gg \frac{\sigma}{2\pi\epsilon} = 10^9 \text{Hz} \quad (52)$$

Therefore at 10^9Hz or $\lambda \ll 30 \text{cm}$, sea water behave as poor conductor. On the other hand at the radio frequency range $f \ll 10^9 \text{Hz}$, the inequality $\sigma \gg \epsilon\omega$, can be satisfied, the skin depth $\delta = \sqrt{2/(\omega\mu\sigma)}$ is quite short. To reach a depth $\delta = 10 \text{m}$, for communication with submarines,

$$f = \frac{\omega}{2\pi} = \frac{1}{\pi\sigma\mu\delta^2} \approx 500 \text{Hz} \quad (53)$$

The wavelength in the air is about

$$\lambda = \frac{c}{f} = \frac{3 \times 10^8}{500} = 600 \text{km} \quad (54)$$

The skin depth at different frequency in sea water are 277 m at 1 Hz, 8.76 m at 1KHz, 0.277 m at 1 MHz and 0.015 at 1GHz if the conductivity of sea-water is taken to about $\sigma = 3/\Omega m$ and $\epsilon_r = 80$. These effects leads to severe restrictions for radio communication with submerged submarines. To overcome this, the communication must be performed with extremely low frequency waves generated by gigantic antennas [47].

9.1 Short wave communications

At 60 km to 100 km height from the earth, ionosphere plasma has a typical density of $10^{13}/\text{m}^3$, which gives the plasma frequency of order 28 MHz. the waves

below this frequency shows reflections from the layer of ionosphere to reach the receiver's end. The conductivity of the earth is 10^{-2} S/m, Earth behave as a good conductor, if the inequality $\sigma \gg \epsilon\omega$ is satisfied. In other word

$$f < \frac{\sigma}{2\pi\epsilon} = 180 \quad (55)$$

MHz, therefore below 20 MHz, the earth is good conductor.

Example: skin depth at $f = 60$ Hz for copper.

$$\delta = \sqrt{\frac{2}{2\pi \times 60 \times 4\pi \times 10^{-7} \times 6 \times 10^7}} = 8\text{mm} \quad (56)$$

The frequency dependent skin-depth in Copper ($\sigma = 6.25 \times 10^7 / \Omega m$) can be expressed as $d = \frac{6}{\sqrt{f(\text{Hz})}}$ cm. It says that the skin-depth is about 6 cm at 1 Hz and it reduced to 2 mm at 1 kHz. In other words it conclude that an oscillating electromagnetic signal of high frequency, transmits along the surface of the wire or on narrow layer of thickness of the order the skin-depth in a conductor. In the visible region ($\omega \sim 10^{15}/s$) of the spectrum, the skin depth for metals is on the order of $10A^0$. The skin depth is related with wavelength λ (inside conductor) as

$$\lambda = \frac{2\pi}{\alpha} = 2\pi\sqrt{\frac{2}{\omega\mu\sigma}} \quad (57)$$

$$\text{The phase velocity } V_{ph} = \frac{\omega}{\alpha} = \frac{\omega\lambda}{2\pi} \approx \sqrt{\frac{2\omega}{\mu\sigma}} \quad (58)$$

Therefore for a very good conductor, the real and imaginary part of the wave vector attain the same values. In this case the amplitude of the wave decays very fast with frequency as compared to bad conductor. The phase velocity of the wave in a good conductor depends on the frequency of the electromagnetic light. Consequently, an electromagnetic wave cannot penetrate more than a few skin-depths into a conducting medium. The skin-depth is smaller at higher frequencies. This implies that high frequency waves penetrate a shorter distance into a conductor than low frequency waves.

Question: Find the skin depths for silver at a frequency of 10^{10} Hz.

$$\text{Skin depth } \delta = \sqrt{\frac{2}{\omega\mu\sigma}} \quad (59)$$

$$\delta = \sqrt{\frac{2}{2\pi \times 10^{10} \times 4\pi \times 10^{-7} \times 6.25 \times 10^7}} = 6.4 \times 10^{-4}\text{mm} \quad (60)$$

Therefore, in microwave experiment, the field do not penetrate much beyond .00064 mm, so no point it's coating making further thicker. There is no advantage to construct AC transmission lines using wires with a radius much larger than the skin depth because the current flows mainly in the outer part of the conductor.

Question: wavelength and propagation speed in copper for radio waves at 1 MHz. compare the corresponding values in air (or vacuum). $\mu_0 = 4\pi \times 10^{-7}$ H/m.

From Eq. (40),

$$\lambda_{Cu} = \frac{2\pi}{\alpha_{Cu}} \text{ and } \alpha_{Cu} \approx \sqrt{\frac{\omega\mu\sigma_{Cu}}{2}} \quad (61)$$

Therefore, $\lambda_{Cu} = 2\pi\sqrt{\frac{2}{\omega\mu\sigma_{Cu}}}$

$$\lambda_{Cu} = 2\pi\sqrt{\frac{2}{2\pi \times 10^6 \times 4\pi \times 10^{-7} \times 6.25 \times 10^7}} = 0.4\text{mm} \quad (62)$$

The propagating velocity in copper $V_{ph} = \frac{\omega}{\alpha} = \frac{\omega\lambda}{2\pi}$

$$V_{ph} = 0.4 \times 10^{-3} \times 10^6 = 400\text{m/s} \quad (63)$$

The above parameters are quite different in vacuum as follow

$$\lambda_{vacuum} = \frac{c}{\nu} = \frac{3 \times 10^8}{10^6} = 300\text{m} \quad (64)$$

There is no advantage to construct AC transmission lines using wires with a radius much larger than the skin depth because the current flows mainly in the outer part of the conductor.

10. Complex permittivity of bread dough and depth of penetration

After baking for few minutes, the relative permittivity of bread dough at frequency 600 MHz is $\epsilon_{cr} = 23.1 - j11.85$. Calculate the depth of penetration of microwave.

Solution: the loss tangent of bread dough is

$$\tan \delta = \frac{11.85}{23.1} = 0.513 \quad (65)$$

The depth of penetration is given as

$$d \approx \frac{c\sqrt{2}}{2\pi f \epsilon_r' \sqrt{(\sqrt{1 + \tan^2 \delta} - 1)}} \quad (66)$$

After substituting all the parameters, we get

$$d \approx \frac{\sqrt{2} \times 3 \times 10^8}{2\pi \times 600 \times 10^6} \frac{1}{23.1 \sqrt{(\sqrt{1 + (0.513)^2} - 1)}} \approx 6.65\text{cm} \quad (67)$$

It is worthy to note that the depth of penetration decreases with frequency.

11. The AC and DC conduction in plasma

Let the collision frequency of electrons with ions and ω the frequency of the EM waves in the conductor. The equation of motion for electrons is:

$$m \frac{dv}{dt} = -eE - m\nu v \quad (68)$$

Assume $v = v_0 e^{-i\omega t}$ and use $\partial/\partial t \rightarrow -i\omega$, we obtain

$$-i\omega m v = -eE - m\nu v \rightarrow v = \frac{-e}{m(\nu - i\omega)} E \quad (69)$$

the current density is expressed by $j = -env$

$$j_f = \frac{-ne^2}{m(\nu - i\omega)} E \quad (70)$$

Therefore, the AC conductivity can be read as

$$\sigma(\omega) = \frac{1}{(\nu - i\omega)} \frac{ne^2}{m} \quad (71)$$

In infrared range $\omega \ll \nu \sim 10^{14}$ (1/sec), so the DC conductivity

$$\sigma = \frac{ne^2}{m\nu} \quad (72)$$

can be taken.

Let us now compare the magnitude of conduction current with that of the displacement current.

Assume $E = E_0 e^{-i\omega t}$. Then

$$\left| \frac{j_f}{\epsilon \frac{\partial E}{\partial t}} \right| = \frac{\sigma E}{\epsilon \omega E} = \frac{\sigma}{\epsilon \omega} \quad (73)$$

In copper, $\sigma = 6 \times 10^7$ (s/m). The condition for $j_f \approx \epsilon \frac{\partial E}{\partial t}$, or $\frac{\sigma}{\epsilon \omega} \approx 1$ leads to

$$\omega = \frac{\sigma}{\epsilon} = \frac{6 \times 10^7}{8.85 \times 10^{-12}} \sim 7 \times 10^{19} \text{ (rad/sec)} \quad (74)$$

At frequencies $\omega < 10^{12}$ (rad/sec) (communication wave frequency),

$$\frac{\sigma}{\epsilon \omega} \gg 1 \text{ or } \left| j_f \right| \gg \left| \epsilon \frac{\partial E}{\partial t} \right|.$$

12. Electromagnetic pulse and high power microwave overview

Several nations and terrorists have a capability to use electromagnetic pulse (EMP) as a weapon to disrupt the critical infrastructures. Electromagnetic pulse is an intense and direct energy field that can interrupt sensitive electrical and electronic equipment over a very wide area, depending on power of the nuclear device and altitude of the burst. An explosion exploded at few heights in the atmosphere can produce EMP and known as high altitude EMP or HEMP. High power microwave (HPM) can be produced with the help of powerful batteries by electrical equipment that transforms battery power into intense microwaves which may be harmful electronics equipments [62–71]. The high- power electromagnetic (HPEM) term describes a set of transient electromagnetic environments with intense electric

and magnetic fields. High- power electromagnetic field may be produced by electrostatic discharge, radar system, lightning strikes, etc. The nuclear bursts can lead to the production of electromagnetic pulse which may be used against the enemy country's military satellites. Therefore the sources derived from lasers, nuclear events are vulnerable and called laser and microwave threats. Microwave weapons do not rely on exact knowledge of the enemy system. These weapons can leave persisting and lasting effects in the enemy targets through damage and destruction of electronic circuits, components. Actually HEMP or HPM energy fields, as they instantly spread outward, may also affect nearby hospital equipment or personal medical devices, such as pacemakers. These may damage critical electronic systems throughout other parts of the surrounding civilian infrastructure. HEMP or HPM may damage to petroleum, natural gas infrastructure, transportation systems, food production, communication systems and financial systems [62–71].

13. Generation of high - frequency instability through plasma environment

The beams of ions and electrons are a source of free energy which can be transferred to high power waves. If conditions are favorable, the resonant interaction of the waves in plasma can lead to nonlinear instabilities, in which all the waves grow faster than exponentially and attain enormously large amplitudes. These instabilities are referred to as explosive instabilities. Such instabilities could be of considerable practical interest, as these seem to offer a mechanism for rapid dissipation of coherent wave energy into thermal motion, and hence may be effective for plasma heating [72, 73]. A consistent theory of explosive instability shows that in the three-wave approximation the amplitudes of all the waves tend to infinity over a finite time called explosion time [74, 75]. In ref. [74], an explosive- generated – plasma is discovered for low and high frequency instabilities. The solution of dispersion equation is found numerically for the possibility of wave triplet and synchronism conditions. The instabilities is observed to propagate whose wave number.

14. Electron beam plasma model and theoretical calculation

Here we considers ions, electrons and negatively charged electron beam are immersed in a Hall thruster plasma channel [51–55]. The magnetic field is consider as $\vec{B} = B\hat{z}$ so that electrons are magnetized while ions remains un-magnetized and electrons rotates with cyclotron frequency $\Omega = \frac{eB}{m_e}$, whereas the gyro-radius for ions is larger so that they cannot rotate and simply ejects out by providing thrust to the device. The axial electric field $\vec{E} = E\hat{x}$ (along the x - axis) which accelerates the particles. It causes electrons have a $\vec{E} \times \vec{B}$ drift in the azimuthal direction (y-axis) whereas the movement of ions is restricted along x-axis. Similar to previous studies, here, we consider the motion of all the species i.e. for ions (density n_i , mass m_i , velocity v_i) for electrons (density n_e , mass m_e , velocity v_e), for electron beam (density n_b , mass m_b , velocity v_b) and collision frequency for the excitation of instability. The basic fluid equations are given as follows:

$$\frac{\partial n_i}{\partial t} + \vec{\nabla} \cdot (\vec{v}_i n_i) = 0 \quad (75)$$

$$m_i \left(\frac{\partial}{\partial t} + (\vec{v}_i \cdot \vec{\nabla}) \right) \vec{v}_i = e \vec{E} \quad (76)$$

$$\frac{\partial n_e}{\partial t} + \vec{\nabla} \cdot (\vec{v}_e n_e) = 0 \quad (77)$$

$$m_e \left(\frac{\partial}{\partial t} + (\vec{v}_e \cdot \vec{\nabla}) + v \right) \vec{v}_e = -e (\vec{E} + \vec{v}_e \times \vec{B}) \quad (78)$$

$$\frac{\partial n_b}{\partial t} + \vec{\nabla} \cdot (\vec{v}_b n_b) = 0 \quad (79)$$

$$m_b \left(\frac{\partial}{\partial t} + (\vec{v}_b \cdot \vec{\nabla}) \right) \vec{v}_b = -e n_b \vec{E} \quad (80)$$

$$\epsilon_0 \nabla^2 \varphi_1 = e(n_{e1} - n_{i1} + n_{b1}) \quad (81)$$

Since the larmor radius of ions are larger than the length of the channel (6 cm), therefore ions are considered as unmagnetized in the channel and are accelerated along the axial direction of the chamber. We consider ions initial drift in the positive x – direction ($\vec{v}_{i0} = v_{i0}\hat{x}$) with neglecting motion in both azimuthal and radial directions [51–55]. Electron has motion in the x -direction ($\vec{v}_b = v_b\hat{x}$) since electrons are affected by magnetic field and get magnetized, we takes their $\vec{E} \times \vec{B}$ initial drift in the y – direction ($\vec{v}_e = v_e\hat{y}$).

To find the oscillations by the solutions of the above equations we take the quantities varied as the $A(r, t) = A_0 e^{i(k \cdot r - \omega t)}$ for first order perturb quantities $n_{i1}, n_{e1}, n_{b1}, v_{i1}, v_{e1}, v_{b1}$ and \vec{E}_1 together with ω as a frequency of oscillations and the k is the wave propagation vector within plane of (x, y). On remarking the magnetic fields are large enough in Hall thruster and condition $\Omega \gg \omega, k_y v_{e0}, v$ is satisfied [51–56]. By solving the equation of motion and the equation of continuity for electrons, we get the perturbed density of electrons in terms of oscillating potential φ_1 in the following way

$$n_{e1} = \frac{e n_{e0} \hat{\omega} k^2 \varphi_1}{m_e \Omega^2 (\omega - k_y v_{e0})} \quad (82)$$

Let us consider, $\hat{\omega} = \omega - k_y v_{e0} - i\nu$, the cyclotron frequency $\Omega = \frac{eB}{m_e}$ and $k^2 = k_x^2 + k_y^2$.

Similarly, on solving equation for ions we get the ion density term as

$$n_{i1} = \frac{e k^2 n_{i0} \varphi_1}{m_i (\omega - k_x v_{i0})^2} \quad (83)$$

Similarly for electron beam density given as

$$n_{b1} = -\frac{e k^2 n_{b0} \varphi_1}{m_b (\omega - k_x v_{b0})^2} \quad (84)$$

By putting these density values in the Poisson's equations

$$-k^2 \varphi_1 = \frac{e^2 n_{e0} \hat{\omega} k^2 \varphi_1}{m_e \epsilon_0 \Omega^2 (\omega - k_y v_{e0})} - \frac{e^2 k^2 n_{i0} \varphi_1}{m_i \epsilon_0 (\omega - k_x v_{i0})^2} - \frac{e^2 k^2 n_{b0} \varphi_1}{m_b \epsilon_0 (\omega - k_x v_{b0})^2} \quad (85)$$

On taking the plasma frequencies as; $\omega_{pe} = \sqrt{\frac{e^2 n_{e0}}{m_e \epsilon_0}}$, $\omega_{pi} = \sqrt{\frac{e^2 n_{i0}}{m_i \epsilon_0}}$, and $\omega_{pb} = \sqrt{\frac{e^2 n_{b0}}{m_b \epsilon_0}}$. Then the above equation reduces in the form as

$$-k^2 \varphi_1 = \frac{\omega_{pe}^2 \hat{\omega} k^2 \varphi_1}{\Omega^2 (\omega - k_y v_{e0})} - \frac{\omega_{pi}^2 k^2 \varphi_1}{(\omega - k_x v_{i0})^2} - \frac{\omega_{pb}^2 k^2 \varphi_1}{(\omega - k_x v_{b0})^2} \quad (86)$$

Since the perturbed potential is not zero i.e. $\varphi_1 \neq 0$ then we get

$$\frac{\omega_{pe}^2 \hat{\omega}}{\Omega^2 (\omega - k_y v_{e0})} - \frac{\omega_{pi}^2}{(\omega - k_x v_{i0})^2} - \frac{\omega_{pb}^2}{(\omega - k_x v_{b0})^2} + 1 = 0 \quad (87)$$

This is the modified dispersion relation for the lower-hybrid waves under the effects of collisions and electrons beam density.

15. Analytical solutions under the limitations

Consider now waves propagating along the \hat{y} direction, so that $k_x = 0$, which, in real thruster geometry, corresponds to azimuthally propagating, waves. We discuss below its limiting cases through Litvak and Fisch [78].

$$\omega \ll |k_y v_{e0}|, \quad (88)$$

The solutions for the dispersion relation (57) can be obtained as follows:

$$\omega^2 \approx \frac{(\omega_{pi}^2 + \omega_{pb}^2) \Omega^2}{(\Omega^2 + \omega_{pe}^2) \left[1 + \frac{i \nu_e \omega_{pe}^2}{(\Omega^2 + \omega_{pe}^2) k_y v_{e0}} \right]} \quad (89)$$

Since the last terms in the second square brackets of the denominator in the right-hand side of (89) are small, we obtain the following

$$\omega \approx \pm \sqrt{\frac{\Omega^2 (\omega_{pi}^2 + \omega_{pb}^2)}{(\Omega^2 + \omega_{pe}^2)}} \left[1 - \frac{i \nu_e \omega_{pe}^2}{2 k_y v_{e0} (\Omega^2 + \omega_{pe}^2)} \right] \quad (90)$$

Finally, the growth rate γ of the resistive instability is calculated from (90) as follow

$$\gamma \approx \frac{\nu_e \omega_{pe}^2}{2 k_y v_{e0} (\Omega^2 + \omega_{pe}^2)} \times \sqrt{\frac{\Omega^2 (\omega_{pi}^2 + \omega_{pb}^2)}{(\Omega^2 + \omega_{pe}^2)}} \quad (91)$$

The corresponding real frequency ω_r ($\omega \equiv \omega_r \pm i\gamma$) is obtained as

$$\omega_r \approx \sqrt{\frac{\Omega^2 (\omega_{pi}^2 + \omega_{pb}^2)}{(\Omega^2 + \omega_{pe}^2)}} \quad (92)$$

The Eqs. (91) show that the growth of the high frequency instability depends on collision frequency, electron density, ion density, beam density, azimuthal wave

Parameters	Range
Magnetic field	$B_{0z} \sim 100 - 200\text{G}$
Axial Wave number	$K_x \sim 200- 600/\text{m}$
Azimuthal Wave number	$K_y \sim 400-1200/\text{m}$
Collisional frequency	$\nu \sim 10^6/\text{s}$
Initial drift of electron	$u_0 \sim 10^6\text{m/s}$
Initial drift of ions	$v_0 \sim 2 \times 10^4 - 5 \times 10^4\text{m/s}$
Plasma density	$n_{e0} \sim 10^{18}, n_{i0} \sim 10^{18}, n_{b0} \sim 10^{17}/\text{m}^3$
Thruster channel diameter	$D \sim 4 - 10 \text{ cm}$

Table 2.
 Plasma parameters.

number, initial drift and on the applied magnetic field. On the other hand, the real frequency of the wave depends only on the magnetic field, electron plasma density, ion density and beam density. By tuning these parameters one can control the frequency of the generating wave. In the below **Table 2**, the different parameters of a Hall thruster are given [51–56].

16. Results and discussion

The Eqs. (91) and (92) are solved with MATLAB by using appropriate parameters given in **Table 2**. We plot various figures for investigating the variation of growth rate and real frequency of the instability with magnetic field B_0 and density of beam n_b , initial drift, collision frequency ν and wave number. For these sets of parameters, only one dominated mode of the dispersion relation is plotted in the figures. **Figure 3** shows the variation of growth rate and real frequency for different values of magnetic field. The reason for the enhanced growth rate as well as real frequency can be understood based on Lorentz force and the electron collisions. Since the electrons have their drift in the y-direction, they experience the Lorentz force due to the magnetic field in the negative of x-direction, i.e., in the direction opposite to the ions drift. The higher Lorentz force helps these transverse oscillations to grow relatively at a faster rate owing to an enhancement in the frequency. On the other hand, this is quite plausible that larger cyclotron frequency of the electrons leads to stronger effects of the collisions because of which the resistive coupling becomes more significant and hence the wave grows at its higher rate. Opposite effect of the magnetic field was observed by Alcock and Keen in case of a drift dissipative instability that occurred in afterglow plasma [76]. Similarly studied are also investigated by Sing and Malik in magnetized plasma [51–56].

In **Figure 4**, we have plotted the variation of growth rate γ and real frequency with the azimuthal wavenumber in order to examine the growth of these waves, when the oscillations are of smaller or relatively longer wavelengths. Here, the oscillations of larger wave numbers (or smaller wavelengths) are found to have lower growth. The faster decay that is observed on the larger side of k is probably due to the stronger Landau damping. The growth rate shows parabolic nature but the real frequency is almost increases linearly with respect to azimuthal wave number. It means that oscillations of smaller wavelengths are most unstable. Kapulkin et al. have theoretically observed the growth rate of instability to directly

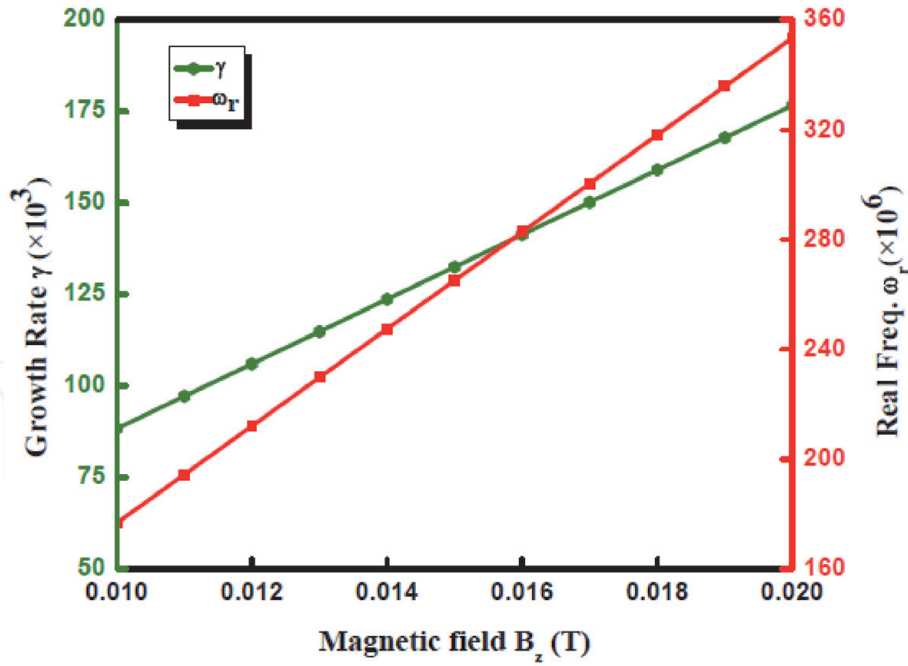


Figure 3.
Variation of growth rate and real frequency with the magnetic field.

proportional to the azimuthal wavenumber [77]. Litvak and Fisch have also shown that the rate of growth of instability is inversely proportional to the azimuthal wave number [78].

On the other hand, the variation of growth rate γ and real frequency with the collision frequency is depicted in **Figure 5**. The wave grow at faster rates in the presence of more electron collisions. This is due to the resistive coupling, which get much stronger in the presence of more collisions. In the present case, the growth rate grows at a much faster rate and real frequency is constant, and graph shows that the growth rate is directly proportional to the collision frequency. During the simulation studies of resistive instability, Fernandez *et al.* also observed the growth

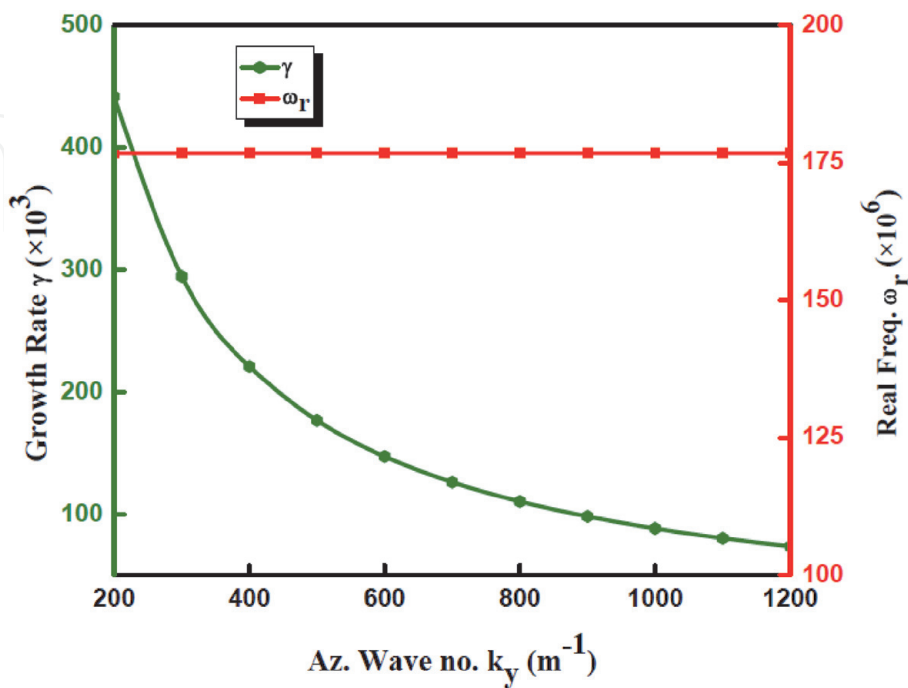


Figure 4.
Variation of growth rate γ and real frequency with azimuthal wavenumber.

rate to be directly proportional to the square root of the collision frequency [79]. In **Figure 6**, we show the dependence of the growth rate on the electron drift velocity. It is observed that the growth rate is reduced in the presence of larger electron drift velocity. In this case the resistive coupling of the oscillations to the electrons' drift would be weaker due to the enhanced velocity of the electrons. The reduced growth under the effect of stronger magnetic field is attributed to the weaker coupling of the oscillations to the electrons closed drift. The variation of growth rate γ and real frequency with beam density are shown in **Figure 7**. The growth shows asymmetric Gaussian type behavior but the real frequency varies linearly with beam density of electrons. This is due to the increased collisional effect with the large plasma density.

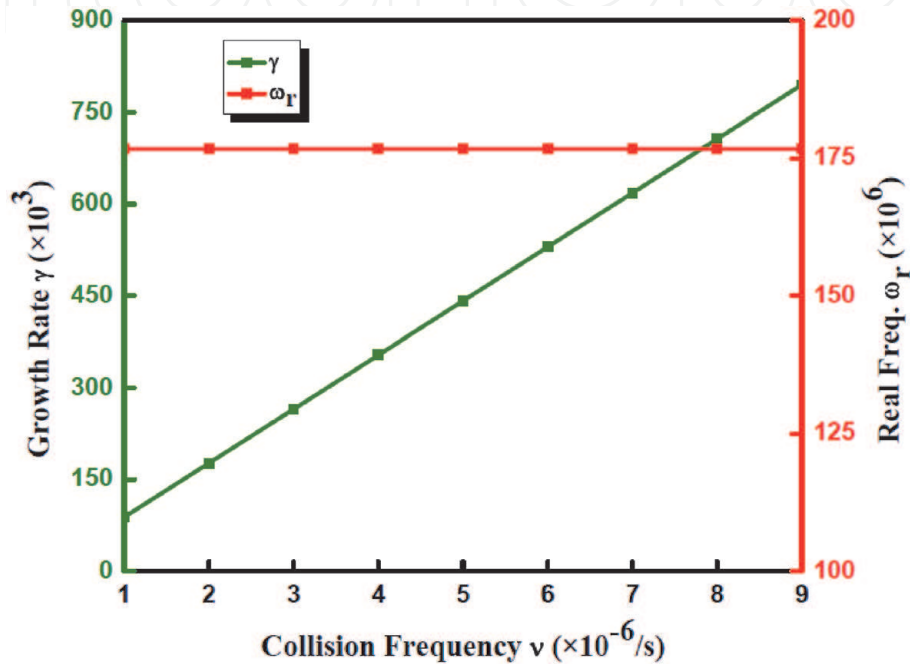


Figure 5.
 Variation of growth rate γ and real frequency with collision frequency.

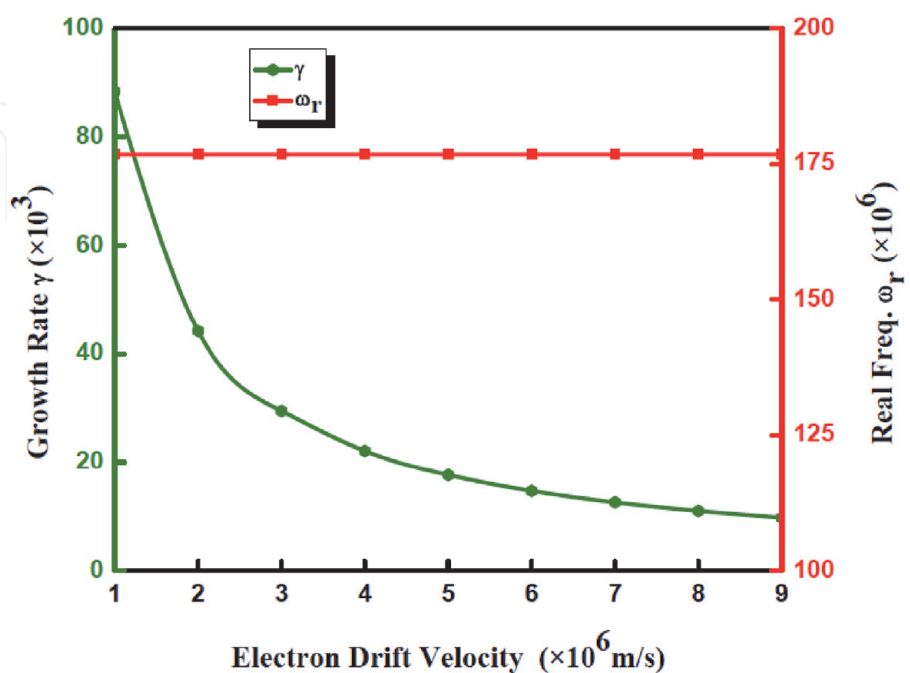


Figure 6.
 Variation of growth rate γ and real frequency with electron drift velocity.

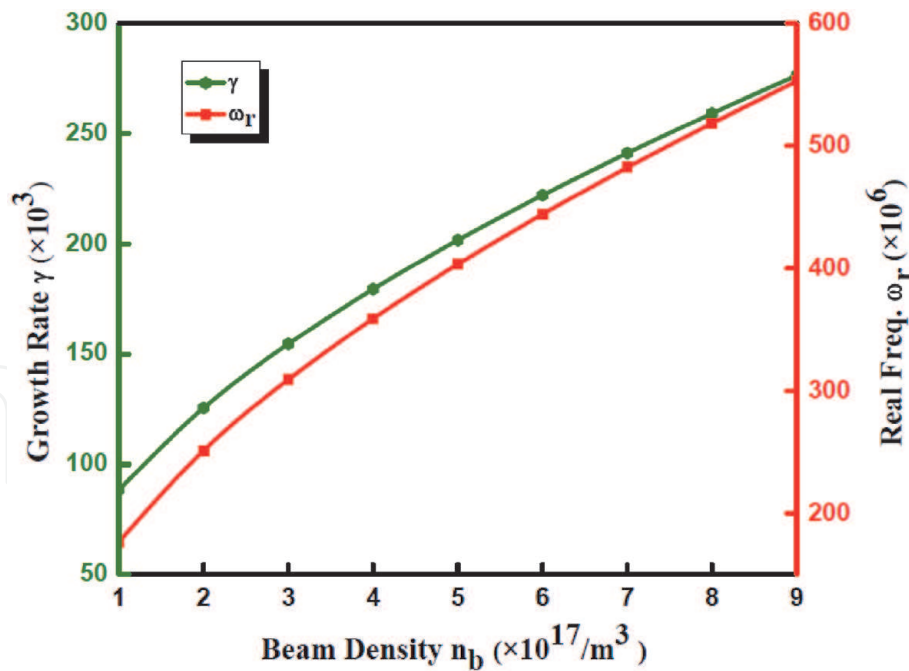


Figure 7.
Variation of growth rate γ and real frequency with beam density.

17. Conclusions

The present chapter discusses the properties of electromagnetic waves propagating through different media. In the first part of the chapter, the dispersion relation for the electromagnetic waves in a conducting medium is derived. It has been experienced that the penetration of the electromagnetic field depends on the frequency of the source as well as the electrical properties of the medium. The significance of skin depth for biological and conducting media is explained through numerical examples. In the second part of the chapter, the generation of high-frequency instability in plasma is discussed, which grows with the magnetic field, wavelength, collision frequency, and the beam density. The growth rate linearly increases with collision frequency of electrons but it decreases with the drift velocity of electrons. The real frequency of the instability increases with magnetic field, azimuthal wave number, and beam density. The real frequency is almost independent with the collision frequency of the electrons.

Acknowledgements

The University Grants Commission (UGC), New Delhi, India is thankfully acknowledged for providing the startup Grant (No. F. 30-356/2017/BSR).

IntechOpen

Author details

Sukhmander Singh^{1*}, Ashish Tyagi² and Bhavna Vidhani³

1 Plasma Waves and Electric Propulsion Laboratory, Department of Physics,
Central University of Rajasthan, Ajmer, Kishangarh, India

2 Physics Department, Swami Shraddhanand College, University of Delhi, Delhi,
India

3 Department of Physics and Electronics, Hansraj College, University of Delhi,
Delhi, India

*Address all correspondence to: sukhmandersingh@curaj.ac.in

IntechOpen

© 2021 The Author(s). Licensee IntechOpen. This chapter is distributed under the terms of the Creative Commons Attribution License (<http://creativecommons.org/licenses/by/3.0>), which permits unrestricted use, distribution, and reproduction in any medium, provided the original work is properly cited. 

References

- [1] L. Liu, S. Zhou and J. Cui, "Prospects and Problems of Wireless Communication for Underwater Sensor Networks," Wiley WCMC Special Issue on Underwater Sensor Networks (Invited), 2008.
- [2] J. H. Goh, A. Shaw, A. I. Al-Shamma'a, "Underwater Wireless Communication System," Journal of Physics, Conference Series 178, 2009.
- [3] A. I. Al-Shamma'a, A. Shaw and S. saman, "Propagation of Electromagnetic Waves at MHz Frequencies through Seawater," IEEE Transactions on Antennas and Propagation, Vol. 52, No. 11, November 2004, pp. 2843-2849.
- [4] S. Bogie, "Conduction and Magnetic Signaling in the Sea," Radio Electronic Engineering, Vol. 42, No. 10, 1972, pp. 447-452. doi:10.1049/ree.1972.0076
- [5] Shan Jiang, Stavros Georgakopoulos, Electromagnetic Wave Propagation into Fresh Water, Journal of Electromagnetic Analysis and Applications, 2011, 3, 261-266
- [6] Habib Mazharimousavi S, Roozbeh A, Halilsoy M. Electromagnetic wave propagation through inhomogeneous material layers. Journal of Electromagnetic Waves and Applications. 2013 Nov 1;27(16): 2065-74.
- [7] Andrey B. Matsko and Yuri V. Rostovtsev, Electromagnetic-wave propagation and amplification in overdense plasmas: Application to free electron lasers, Physical Review E, 58, 6, DECEMBER 1998
- [8] P. Sprangle, E. Esarey, J. Krall, and G. Joyce, Phys. Rev. Lett. 69, 2200 ~1992.
- [9] .C. Oldano, Electromagnetic-wave propagation in anisotropic stratified media, Physical Review A, 40, 10 NOVEMBER 15, 1989
- [10] Hidenori Akiyama, Takashi Sakugawa, Takao Namihira, Industrial Applications of Pulsed Power Technology, IEEE Transactions on Dielectrics and Electrical Insulation Vol. 14, No. 5; October 2007, 1051-1064
- [11] A. Pokryvailo, M. Wolf, Y. Yankelevich, S. Wald, L. R. Grabowski, E. M. van Veldhuizen, Wijnand R. Rutgers, M. Reiser, B. Glocker, T. Eckhardt, P. Kempenaers and A. Welleman, "High-Power Pulsed Corona for Treatment of Pollutants in Heterogeneous Media", IEEE Trans. Plasma Sci., Vol. 34, pp. 1731-1743, 2006.
- [12] G.J.J. Winands, K. Yan, A.J.M. Pemen, S.A. Nair, Z. Liu and E.J.M. vanHeesch, "An Industrial Streamer Corona Plasma System for Gas Cleaning", IEEE Trans. Plasma Sci., Vol. 34, pp.2426-2433, 2006.
- [13] W. Hartmann, T. Hammer, T. Kishimoto, M. Romheld and A. Safitri, "Ozone Generation in a Wire-Plate Pulsed Corona Plasma Reactor", 15th IEEE Pulsed Power Conf., pp. 856-859, 2005.
- [14] J. Choi, T. Yamaguchi, K. Yamamoto, T. Namihira, T. Sakugawa, S. Katsuki and H. Akiyama, "Feasibility Studies of EMTP Simulation for the Design of the Pulsed-Power Generator Using MPC and BPFN for Water Treatments", IEEE Trans. Plasma Sci., Vol. 34, pp.1744-1750, 2006.
- [15] R.W. Bruce, R.L. Bruce, A.W. Fliflet, M. Kahn, S.H. Gold, A.K. Kinkead, D. Lewis, III and M.A. Imam, "Joining of ceramic tubes using a high-power 83-GHz Millimeter-wave beam", IEEE Trans. Plasma Sci., Vol. 33, pp. 668-678, 2005.

- [16] A. M. Loske, "Medical and Biomedical Applications of Shock Waves: The State of the Art and the Near Future," in 30th International Symposium on Shock Waves 1, 2017, pp. 29-34.
- [17] Claire M. Watts, Xianliang Liu, and Willie J. Padilla, *Metamaterial Electromagnetic Wave Absorbers*, *Adv. Mater.* 2012, 24, OP98–OP120, DOI: 10.1002/adma.201200674
- [18] A. I. M. Ayala, Master of Science Thesis, Tufts University, USA, 2009.
- [19] Y. Gong, Z. Li, J. Fu, Y. Chen, G. Wang, H. Lu, L. Wang, X. Liu, *Opt. Exp.* 2011, 19, 10193
- [20] Z. H. Jiang, S. Yun, F. Toor, D. H. Werner, T. S. Mayer, *ACS Nano* 2011, 5, 4641.
- [21] X. J. He, Y. Wang, J. M. Wang, T. L. Gui, *PIER* 2011, 115, 381
- [22] E. Berry et al., "Optical properties of tissue measured using terahertz-pulsed imaging," *Proc. SPIE*, vol. 5030, pp. 459-470, Jun. 2003.
- [23] A. J. Fitzgerald et al., "Catalogue of human tissue optical properties at terahertz frequencies," *J. Biol. Phys.*, vol. 29, nos. 2-3, pp. 123-128, 2003.
- [24] G. W. Hanson, "Dyadic Green's functions and guided surface waves for a surface conductivity model of graphene," *J. Appl. Phys.*, vol. 103, no. 6, pp. 064302-1–064302-8, Mar. 2008.
- [25] J. M. Jornet and I. F. Akyildiz, "Graphene-based nano-antennas for electromagnetic nanocommunications in the terahertz band," in *Proc. 4th Eur. Conf. Antennas Propag. (EUCAP)*, Apr. 2010, pp. 1-5.
- [26] T. Binzoni, A. Vogel, A. H. Gandjbakhche, and R. Marchesini, "Detection limits of multi-spectral optical imaging under the skin surface," *Phys. Med. Biol.*, vol. 53, no. 3, pp. 617-636, 2008.
- [27] Loske, A.M.: *Medical and Biomedical Applications of Shock Waves. Shock Wave and High Pressure Phenomena*. Springer International Publishing AG, Cham, Switzerland (2017). ISBN 978-3-319-47568-4
- [28] Wang, C.J.: "Extracorporeal shockwave therapy in musculoskeletal disorders." *J. Orthop. Surg. Res.* 7, 11–17 (2012)
- [29] Kenmoku, T., Nobuyasu, O., Ohtori, S.: "Degeneration and recovery of the neuromuscular junction after application of extracorporeal shock wave therapy." *J. Orthop. Res.* 30, 1660–1665 (2012)
- [30] Delius, M., Hofschneider, P.H., Lauer, U., Messmer, K. "Extracorporeal shock waves for gene therapy?" *Lancet* 345, 1377 (1995)
- [31] Chen ZY, Gao YM, Du M. "Propagation characteristics of electromagnetic wave on multiple tissue interfaces in wireless deep implant communication." *IET Microwaves, Antennas & Propagation*. 2018 Jul 6;12 (13):2034-40.
- [32] Callejon, M.A., Naranjo-Hernandez, D., Reina-Tosina, J. and Roa LM, "Distributed circuit modeling of galvanic and capacitive coupling for intrabody communication", *IEEE Trans. Biomed. Eng.*, 2012, 59, (11), pp. 3263– 3269
- [33] Seyedi M, Kibret B, Lai DT and Faulkner M. "A survey on intrabody communications for body area network applications", *IEEE Trans. Biomed. Eng.*, 2013, 60, (8), pp. 2067– 2079
- [34] Marani R, Perri AG. "RFID technology for biomedical applications: State of art and future developments." *i-Manager's Journal on Electronics Engineering*. 2015 Dec 1;6(2):1.

- [35] A. Denisov and E. Yeatman, "Ultrasonic vs. inductive power delivery for miniature biomedical implants," in *Body Sensor Networks (BSN)*, 2010 International Conference on, 2010, pp. 84-89: IEEE.
- [36] S. Ozeri and D. Shmilovitz, "Ultrasonic transcutaneous energy transfer for powering implanted devices," *Ultrasonics*, vol. 50, no. 6, pp. 556-566, 2010.
- [37] Li C, Un KF, Mak PI, Chen Y, Muñoz-Ferreras JM, Yang Z, Gómez-García R. Overview of recent development on wireless sensing circuits and systems for healthcare and biomedical applications. *IEEE Journal on Emerging and Selected Topics in Circuits and Systems*. 2018 Apr 3;8(2): 165-77.
- [38] R. Muller et al., "A minimally invasive 64-channel wireless μ ECoG implant," *IEEE Journal of Solid-State Circuits*, vol. 50, no. 1, pp. 344-359, 2015.
- [39] G. Papotto, F. Carrara, A. Finocchiaro, and G. Palmisano, "A 90nm CMOS 5Mb/s crystal-less RF transceiver for RF-powered WSN nodes," in *Solid-State Circuits Conference Digest of Technical Papers (ISSCC)*, 2012 IEEE International, 2012, pp. 452-454: IEEE.
- [40] Z.-P. Liang and P. C. Lauterbur, *Principles of magnetic resonance imaging: a signal processing perspective*. SPIE Optical Engineering Press, 2000.
- [41] P. Lauterbur, "Image formation by induced local interactions: examples employing nuclear magnetic resonance," 1973.
- [42] S. Gabriel, R. Lau, and C. Gabriel, "The dielectric properties of biological tissues: III. Parametric models for the dielectric spectrum of tissues," *Physics in medicine and biology*, vol. 41, no. 11, p. 2271, 1996.
- [43] C. Gabriel, S. Gabriel, and E. Corthout, "The dielectric properties of biological tissues: I. Literature survey," *Physics in medicine and biology*, vol. 41, no. 11, p. 2231, 1996.
- [44] S. Gabriel, R. Lau, and C. Gabriel, "The dielectric properties of biological tissues: II. Measurements in the frequency range 10 Hz to 20 GHz," *Physics in medicine and biology*, vol. 41, no. 11, p. 2251, 1996.
- [45] Johnson C C and Guy AW, *Nonionizing Electromagnetic Wave Effects in Biological Materials and Systems*, *Proceedings of THE IEEE*, VOL. 60, NO. 6, J ~ T E(19 72)692-718
- [46] C. J. Restall, P. F. Leonard, H. F. Taswell, and R. E. Holaday. *IMPI Symp.* (Univ. of Alberta, Edmonton, Canada, May 21-"Warming of human blood by use of microwaves," in *Summ. 4th*, 23, 1969), pp. 9699.
- [47] Inan US, Said RK and Inan AS. *Engineering electromagnetics and waves*. Pearson; 2014 Mar 14.
- [48] David J. Griffiths *Introduction to Electrodynamics*. (Addison-Wesley: Upper Saddle River, 1999).
- [49] Jackson, J. D. (1998). *Classical Electrodynamics*. New York: Wiley, 3rd edition
- [50] Mallick C, Bandyopadhyay M, Kumar R. Evolution of Microwave Electric Field on Power Coupling to Plasma during Ignition Phase. *InSelected Topics in Plasma Physics 2020 Jun 15. IntechOpen*.
- [51] Tyagi J, Singh S, Malik HK, Effect of dust on tilted electrostatic resistive instability in a Hall thruster. *Journal of Theoretical and Applied Physics*. 2018; 12: 39-43. Doi.org/10.1007/s40094-018-0278-z
- [52] Singh S, Malik H K, Nishida Y. High frequency electromagnetic resistive

instability in a Hall thruster under the effect of ionization. *Physics of Plasmas*.2013; 20: 102109 (1-7).

[53] Singh S, Malik H K. Growth of low frequency electrostatic and electromagnetic instabilities in a Hall thruster. *IEEE Transactions on Plasma Science*.2011; 39:1910-1918.

[54] Singh S, Malik H K. Resistive instabilities in a Hall thruster under the presence of collisions and thermal motion of electrons. *The Open Plasma Physics Journal*. 2011; 4:16-23.

[55] Malik H K and Singh S. Resistive instability in a Hall plasma discharge under ionization effect. *Physics of Plasmas*.2013; 20: 052115 (1-8).

[56] Singh S. Evolutions of Growing Waves in Complex Plasma Medium. In edited book *Engineering Fluid Mechanics*. IntechOpen, London, United Kingdom, Nov 2020

[57] Singh S. Waves and Instabilities in E X B Dusty Plasma. In the edited book *Thermophysical Properties of Complex Materials*. IntechOpen, London, United Kingdom, December 12th 2019

[58] Singh S. Dynamics of Rayleigh-Taylor Instability in Plasma Fluids. In the edited book *Engineering Fluid Mechanics*. IntechOpen, London, United Kingdom, April 15th 2020

[59] Singh S. Hall Thruster: An Electric Propulsion through Plasmas. In the edited book *Plasma Science* IntechOpen, London, United Kingdom, March 2nd 2020 Doi.org/10.1063/1.2823033

[60] Singh S, Kumar S, Sanjeev, Meena S K and Saini S K. Introduction to Plasma Based Propulsion System: Hall Thrusters. In the edited book *Propulsion - New Perspectives and Applications*" edited by Prof. Kazuo Matsuuchi, IntechOpen, London, United Kingdom, March 2021

[61] Singh S, editor. *Selected Topics in Plasma Physics*. BoD–Books on Demand; 2020 Nov 19.

[62] Khalatpour A, Paulsen AK, Deimert C, Wasilewski ZR, Hu Q. High-power portable terahertz laser systems. *Nature Photonics*. 2021 Jan;15(1):16-20.

[63] Wu S, Cui S. Overview of High-Power Pulsed Power Supply. In *Pulsed Alternators Technologies and Application 2021* (pp. 1-35). Springer, Singapore.

[64] Wu S, Cui S. Electromagnetic Weapon Load of Pulsed Power Supply. In *Pulsed Alternators Technologies and Application 2021* (pp. 209-227). Springer, Singapore.

[65] Radasky, W. A., C. E., Baum, Wik, M. W.: Introduction to the special issue on high power electromagnetics (HPEM) and intentional electromagnetic interference (IEMI) environments and test capabilities. *IEEE Trans. Electromagn. Compat.* 46 (2004)

[66] Sabath, F., Backstrom, M., Nordstrom, B., Serafin, D., Kaiser, A., Kerr, B., Nitsch, D.: Overview of four European high power microwave narrow band test facilities. *IEEE Trans. Electromagn. Compat.* 46, 329 (2004)

[67] Parfenov, Y. V., Zdoukhov, L. N., Radasky, W. A., Ianoz, M.: Conducted IEMI threats for commercial buildings. *IEEE Trans. Electromagn. Compat.* 46, 404 (2004)

[68] Lu X, Picard JF, Shapiro MA, Mastovsky I, Temkin RJ, Conde M, Power JG, Shao J, Wisniewski EE, Peng M, Ha G. Coherent high-power RF wakefield generation by electron bunch trains in a metamaterial structure. *Applied Physics Letters*. 2020 Jun 29;116 (26):264102.

[69] Zhang J, Zhang D, Fan Y, He J, Ge X, Zhang X, Ju J, Xun T. Progress in

narrowband high-power microwave sources. *Physics of Plasmas*. 2020 Jan 17; 27(1):010501.

[70] Frank JW. Electromagnetic fields, 5G and health: what about the precautionary principle?. *J Epidemiol Community Health*. 2021 Jun 1;75(6): 562-6.

[71] Wu S, Cui S. Basic Theories of Pulsed Alternators. In *Pulsed Alternators Technologies and Application 2021* (pp. 37-61). Springer, Singapore.

[72] Aamodt, R. E., Sloan, M. L.: Nonlinear interactions of positive and negative energy waves. *Phys. Fluids* 11, 2218 (1968)

[73] Wilhelmson, H., Stenflo, I., Engelmann, F.: Explosive instabilities in the well defined phase description. *J. Math. Phys.* 11, 1738 (1970)

[74] O.P. Malik, Sukhmander Singh, Hitendra K. Malik, A. Kumar. Low and high frequency instabilities in an explosion-generated-plasma and possibility of wave triplet. *Journal of Theoretical and Applied Physics* (2015) Vol. 9 Pgs.75 -80.

[75] O.P. Malik, Sukhmander Singh, Hitendra K. Malik, A. Kumar. High frequency instabilities in an explosion-generated-relativistic-plasma. *Journal of Theoretical and Applied Physics* (2015) Vol. 9, Pgs.105-110.

[76] Alcock M W & Keen B E, *Phys Rev A* 3, (1971) 1087.

[77] Kapulkin A, Kogan A & Guelman M, *Acta Astronaut*, 55 (2004) 109.

[78] Litvak A A & Fisch N J, *Phys Plasmas*, 8 (2001) 648.

[79] Fernandez E, Scharfe MK, Thomas CA, Gascon N & Cappelli MA, *Phys Plasmas*, 15, 012102 (2008).